Dalton Transactions

RSC Publishing

PAPER

View Article Online
View Journal | View Issue

Cite this: *Dalton Trans.*, 2013, **42**, 16510

From antiferromagnetic to ferromagnetic exchange in a family of oxime-based Mn^{III} dimers: a magneto-structural study†‡

Wdeson P. Barros,[a,b] Ross Inglis,[a] Gary S. Nichol,[a] Thayalan Rajeshkumar,[c] Gopalan Rajaraman,*[c] Stergios Piligkos,[d] Humberto O. Stumpf*[b] and Euan K. Brechin*[a]

Received 26th July 2013,
Accepted 22nd August 2013

DOI: 10.1039/c3dt52009a

www.rsc.org/dalton

The reaction of $Mn(ClO_4)_2{\cdot}6H_2O$, a derivatised phenolic oxime (R-saoH$_2$) and the ligand tris(2-pyridylmethyl)amine (tpa) in a basic alcoholic solution leads to the formation of a family of cluster compounds of general formula $[Mn^{III}_2O(R\text{-}sao)(tpa)_2](ClO_4)_2$ (**1**, R = H; **2**, R = Me; **3**, R = Et; **4**, R = Ph). The structure is that of a simple, albeit asymmetric, dimer of two Mn^{III} ions bridged through one $\mu\text{-}O^{2-}$ ion and the –N–O– moiety of the phenolic oxime. Magnetometry reveals that the exchange interaction between the two Mn^{III} ions in complexes **1**, **3** and **4** is antiferromagnetic, but that for complex **2** is ferromagnetic. A theoretically developed magneto-structural correlation reveals that the dominant structural parameter influencing the sign and magnitude of the pairwise interaction is the dihedral Mn–O–N–Mn (torsion) angle. A linear correlation is found, with the magnitude of *J* varying significantly as the dihedral angle is altered. As the torsion angle increases the AF exchange decreases, matching the experimentally determined data. DFT calculations reveal that the $d_{yz}|\pi^*|d_{yz}$ interaction decreases as the dihedral angle increases leading to ferromagnetic coupling at larger angles.

Introduction

The physical properties of polymetallic molecular cages, constructed from paramagnetic d- or f-block metal ions, continue to fascinate chemists and physicists alike.[1–20] These molecules, often referred to in the most general sense as *molecular nanomagnets*, have been proposed for application in information storage, spintronics, quantum computation and low temperature magnetic refrigeration.[21–26] Of course any such application first requires the academic foundations to be laid down, and this means examining, understanding and ultimately exploiting the fundamental relationship between structure and magnetic behaviour, ideally in a (large) family of closely related complexes. The inherent complexity in the structures of large cluster compounds, that often possess low symmetry, is however an obstacle to extracting pertinent quantitative data.[27] A multitude of different exchange interaction pathways borne from, for example, two or more ligand types, diverse ligand coordination and bridging modes, the innocence or non-innocence of co-ligands, and the presence of more than one metal type or mixed valency in the same metal type, often render a detailed quantitative analysis impossible, resulting in a more qualitative description in which numerous assumptions are required for the sake of simplicity and the avoidance of over-parameterisation.[28–34] A long-employed method to combat such problems is the synthesis of small molecules whose structures are analogous to the building blocks observed in larger cages. For example, large Mn^{III} clusters are commonly built upon shared $[Mn_3O]^{n+}$ triangles and/or $[Mn_4O_2]^{n+}$ butterflies.[35] Examination of the effect on the nature and magnitude of magnetic exchange on changing, for example, the bridging ligand type, the metal–metal separation, the bond angles subtended at the bridging atoms, the dihedral angles between coordination planes containing the metal ions, the metal–ligand bond lengths, the metal ion stereochemistries, can therefore provide valuable information on what structural parameters dominate the magnetism.[28–34]

[a]*EaStCHEM School of Chemistry, The University of Edinburgh, West Mains Road, Edinburgh, EH9 3JJ, UK. E-mail: ebrechin@staffmail.ed.ac.uk*
[b]*Departamento de Química, ICEx, Universidade Federal de Minas Gerais, Av. Antônio Carlos 6627, Belo Horizonte-MG, 31270-901, Brazil. E-mail: stumpf@ufmg.br*
[c]*Department of Chemistry, Indian Institute of Technology Bombay, Powai, Mumbai, 400076, India. E-mail: rajaraman@chem.iitb.ac.in*
[d]*Department of Chemistry, University of Copenhagen, Universitetsparken 5, DK-2100, Denmark. E-mail: piligkos@kiku.dk*

† Celebrating 300 years of chemistry at The University of Edinburgh.

‡ Electronic supplementary information (ESI) available: Computed overlap integrals and spin densities for complexes **1–4**. CCDC 950511–950514. For ESI and crystallographic data in CIF or other electronic format see DOI: 10.1039/c3dt52009a

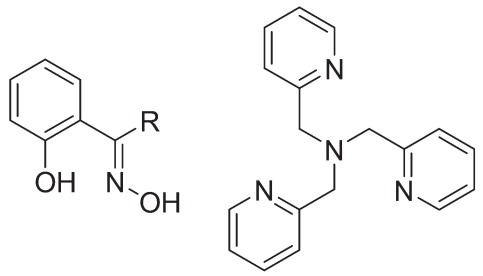

Scheme 1 The structures of R-saoH$_2$ (left, R = H, saoH$_2$; R = Me, Me-saoH$_2$; R = Et, Et-saoH$_2$; R = Ph, Ph-saoH$_2$) and tpa (right).

A highly promising family of ligands for constructing magnetically interesting clusters based on Mn^{III} are the phenolic oximes (R-saoH$_2$, Scheme 1).[36] In basic alcoholic solutions the Mn^{III}/R-saoH$_2$ reaction mixture generally affords molecules containing the triangular $[Mn^{III}_3O(R\text{-}sao)_3]^+$ building block.[37] Nearest neighbour magnetic exchange is dominated by the twisting of the –N–O– moiety of the phenolic oxime and the sign and magnitude of the pairwise exchange can be controlled *via* chemical substitution at the oximic C-atom.[38] The Mn^{III}/R-sao^{2-} (Mn–O–N–Mn) moiety therefore represents a potentially interesting building block for functional materials, but while magneto-structural correlations have been investigated for the triangular $[Mn^{III}_3O(R\text{-}sao)_3]^+$ building block,[39] there is a dearth of examples in the literature of molecules containing alternative topologies.[40–42] Our most recent research attempts have therefore focused on deliberately targeting Mn^{III} clusters with the R-saoH$_2$ family of ligands whose building blocks are *not* $[Mn^{III}_3O(R\text{-}sao)_3]^+$ triangles. Our initial approach is simple and threefold: (a) use solvents other than ROH, (b) employ co-ligands that are able to compete with the oximes for the metal coordination sites, and (c) make heterometallic clusters in which the second [dia or paramagnetic] metal ion does not favour the formation of the oxo-centred triangles. This has already borne some success with the synthesis of a $[Mn_{32}]$ double-decker wheel,[40] homo- and heterometallic dimers,[41] and a family of $[Mn^{III}_6Ln^{III}_2]$ hexagonal prisms.[42]

A simple method for favouring the formation of smaller clusters is through the use of polydentate chelating ligands which occupy the majority of coordination sites on the metal centre, leaving only one or two vacant sites for bridging ligands. An excellent candidate in this regard is the tripodal tetradentate ligand tris(2-pyridylmethyl)amine (tpa) which has been used extensively to obtain dimers and trimers of Cu^{II},[43–45] Fe^{III},[46,47] Cr^{II} and Cr^{III},[48–51] Co^{II}, Ni^{II},[52,53] Mn^{II} and Mn^{III}.[54–56] This ligand contains a tertiary N-atom bonded to three arms, each of which contains an N-donor atom from a pyridine ring (Scheme 1). While the tpa ligand has been widely used for the construction of functional models for various non-heme iron mono-oxygenases and other oxygen-activating enzymes,[57–59] its use in Mn chemistry has been more limited. Herein, we report the synthesis and magnetic characterisation of a new family of Mn^{III} dinuclear complexes of general formula $[Mn^{III}_2O(R\text{-}sao)(tpa)_2](ClO_4)_2$ (where R = H, Me, Et, Ph).

Experimental

Materials and physical measurements

All manipulations were carried out under aerobic conditions using materials as received (reagent grade). **Caution!** Although no problems were encountered in this work, care should be taken when using the potentially explosive perchlorate anion. The substituted oximes, R-saoH$_2$, (R = Me, Et, Ph) were synthesised by the reaction of the appropriate precursor ketones with hydroxylamine and sodium acetate in EtOH, as described in the literature.[60] Variable temperature, solid-state magnetic susceptibility data down to 5 K were collected on a Quantum Design MPMS-XL SQUID magnetometer equipped with a 7 T dc magnet. Diamagnetic corrections were applied to the observed paramagnetic susceptibilities using Pascal's constants.

Synthesis

General procedure for $[Mn^{III}_2O(R\text{-}sao)(tpa)_2](ClO_4)_2$ (**1**, R = H; **2**, R = Me; **3**, R = Et; **4**, R = Ph). $Mn(ClO_4)_2{\cdot}6H_2O$ (0.4 mmol), R-saoH$_2$ (0.4 mmol) and Et_3N (1.6 mmol) were dissolved in MeOH (10 mL) and stirred for 30 minutes at room temperature. To the resulting solution was added tpa (0.4 mmol) in EtOH (10 mL), followed after 5 minutes by paper filtration. Diethyl ether was then diffused into the resulting solution. Dark green/brown crystals suitable for X-ray diffraction formed after ~1 week. Elemental analyses, calculated (found). **1**: C 49.20(48.58), H 4.03(3.73), N 12.01(11.37). **2**: C 49.84(49.01), H 4.15(3.81), N 11.89(11.22). **3**: C 50.57(49.98), H 4.24(4.24), N 11.80(11.16). **4**: C 52.49(52.06), H 4.18(4.27), N 11.13(10.55).

X-ray crystallography

Diffraction data were collected at 120 K (**1**, **2** and **4**) on an Agilent Technologies SuperNova diffractometer and at 170 K (**3**) on an Agilent Technologies XCalibur diffractometer, using Mo-Kα and Cu-Kα radiation. Each data reduction and absorption corrections were carried out on the CrysAlisPro software package. The structures were solved using the charge-flipping algorithm (SUPERFLIP)[61] and refined by full matrix least squares using SHELXL-97.[62] All C-bonded hydrogen atoms were modelled isotropically and assigned to idealised positions. Data collection parameters, structure solution and refinement details are listed in Table 1 and CCDC 950511–950514.

Computational details

All calculations were performed using the hybrid B3LYP[63] functional with Alhrich's[64] triple-ζ basis set as implemented in the Gaussian 09[65] suite of programs. The *J* values were computed from the energy differences between the high spin (E_{HS}) state calculated using single determinant wave functions, and the low spin (E_{BS}) state determined using the Broken Symmetry (BS) approach developed by Noodleman.[66] Negative and positive values for *J* correspond to antiferromagnetic and ferromagnetic interactions, respectively. Details of the computational methodology employed to compute the exchange interaction is discussed elsewhere.[67]

Table 1 Crystallographic data for complexes **1**·0.5H_2O, **2**·0.32H_2O, **3** and **4**·0.5MeOH

	1·0.5H_2O	**2**·0.32H_2O	**3**	**4**·0.5MeOH
Formula[a]	$C_{86}H_{84}Cl_4Mn_4N_{18}O_{23}$	$C_{44}H_{43.64}Cl_2Mn_2N_9O_{11.32}$	$C_{45}H_{45}Cl_2Mn_2N_9O_{11}$	$C_{99}H_{94}Cl_4Mn_4N_{18}O_{23}$
M_W	2099.27	1060.42	1068.68	2265.48
Crystal system	$P\bar{1}$	$P\bar{1}$	$P\bar{1}$	$P2_1/c$
Space group	Triclinic	Triclinic	Triclinic	Monoclinic
a/Å	10.7837(3)	10.7046(4)	11.0368(4)	11.3801(2)
b/Å	11.6961(4)	11.6206(4)	11.5272(6)	22.7282(4)
c/Å	18.9210(6)	19.4847(6)	19.2934(10)	19.6458(4)
α (°)	73.692(3)	74.968(3)	74.555(5)	90
β (°)	80.838(3)	79.750(3)	81.387(4)	97.4164(16)
γ (°)	88.509(3)	89.644(3)	84.794(4)	90
V/Å^3	2260.79(12)	2301.46(14)	2335.92(19)	5038.87(16)
Z	1	2	2	2
T/K	120(2)	120(2)	170(2)	120(2)
λ[b]/Å	1.54184	1.54184	0.71073	0.71073
D_c/g cm^{-3}	1.542	1.530	1.519	1.493
μ/mm^{-1}	6.248	6.141	0.726	0.678
Meas./indep. (R_{int}) refl.	25 644/8930 (0.0283)	36 643/9143 (0.0405)	28 621/6699 (0.0528)	41 286/11 501 (0.0447)
Obs. refl. [$I > 2\sigma(I)$]	7758	7880	5042	8573
wR_2 [c,d]	0.0855	0.1242	0.0732	0.0927
R_1 [d,e]	0.0348	0.0484	0.0412	0.044
Goodness of fit on F^2	1.012	1.015	1.019	1.047
$\Delta\rho_{max,min}$/e Å^{-3}	0.674/−0.554	0.969/−1.090	0.334/−0.281	0.588/−0.420

[a] Including solvate molecules. [b] Cu Kα (**1**, **2**) and Mo Kα (**3**, **4**) radiation. [c] $wR_2 = [\sum w(|F_o^2| - |F_c^2|)^2/\sum w|F_o^2|^2]^{1/2}$. [d] For observed data. [e] $R_1 = \sum||F_o| - |F_c||/\sum|F_o|$.

Results and discussion

The reaction between $Mn(ClO_4)_2$·6H_2O, the appropriately substituted phenolic oxime (R-saoH_2 where R = H, Me, Et or Ph) and Et_3N in the presence of the tripodal tetradentate ligand tpa affords complexes **1–4**, which were crystallographically identified as $[Mn^{III}_2O(sao)(tpa)_2](ClO_4)_2$·0.5$H_2O$ (**1**·0.5H_2O); $[Mn^{III}_2O(Me\text{-}sao)(tpa)_2](ClO_4)_2$·0.32$H_2O$ (**2**·0.32H_2O); $[Mn^{III}_2O(Et\text{-}sao)(tpa)_2](ClO_4)_2$ (**3**); and $[Mn^{III}_2O(Ph\text{-}sao)(tpa)_2](ClO_4)_2$·0.5MeOH (**4**·0.5MeOH). All four complexes display very similar structures (Fig. 1, Tables 1 and 2) with **1–3** crystallising in the triclinic space group $P\bar{1}$ and **4** in the monoclinic space group $P2_1/c$. For the sake of brevity we provide a generic structure description, highlighting any differences. Relevant interatomic distances and angles are given in Table 2.

The structure describes a simple, albeit asymmetric, dimer in which two Mn^{III} ions are bridged by one μ-O^{2-} ion (Mn1–O3–Mn2, 120.73° (**1**); 119.45° (**2**); 119.98° (**3**); 120.20° (**4**)) and the –N–O– moiety of the phenolic oxime (Mn1–O2–N1–Mn2, 8.36° (**1**); 13.55° (**2**); 12.92° (**3**); 8.84° (**4**)). The two tpa ligands are of two types: Mn1 is coordinated by a κ^4-ligand in which all four N-atoms are bonded to the metal centre, while Mn2 is coordinated by a κ^3-ligand, in which one of the pyridine arms remains uncoordinated (N9). The average Mn1–N_{amine} distance is ~2.16 Å, which is slightly shorter than the average Mn2–N_{amine} distance of ~2.24 Å, likely reflecting the change in denticity of the ligand. The average Mn1–N_{pyr} distance for the nitrogen atom *trans* to the μ-O^{2-} ion (~2.06 Å), is somewhat shorter than the other Mn1–N_{pyr} bonds (~2.26 Å). Furthermore, the average Mn2–N_{oxime} bond length of ~2.03 Å is appreciably shorter than the average Mn2–N_{pyr} distance of ~2.25 Å. Both Mn^{III} ions are in distorted octahedral geometries with the expected Jahn–Teller elongation along the N7···N8 vector for Mn2, and the N3···N4 vector for Mn1. The Mn1···Mn2 distances are 3.135 Å (**1**), 3.114 Å (**2**), 3.123 Å (**3**) and 3.122 Å (**4**). There are no intermolecular H-bonding interactions in the packing of **1–4** with the closest intermolecular interactions being of the order of ~3.4 to ~3.8 Å between the C-atoms of the oxime/tpa ligands.

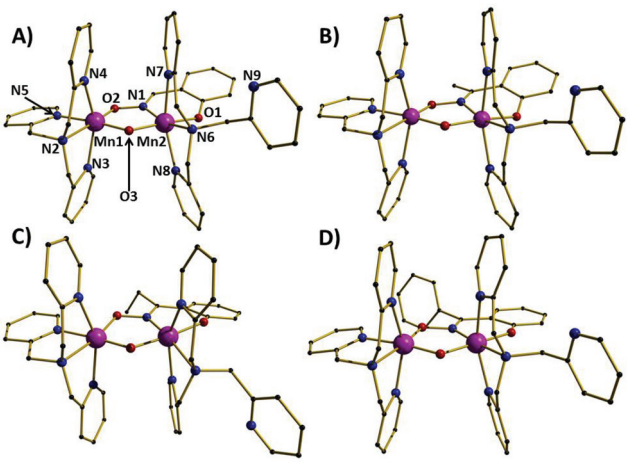

Fig. 1 The molecular structures of **1–4** (A–D), respectively. Colour code: Mn = purple, O = red, N = blue, C = black. H-atoms, counter ions and solvent molecules are omitted for clarity.

Magnetic behaviour

The dc molar magnetic susceptibilities, χ_M, of polycrystalline samples of **1–4** were measured in an applied magnetic field, B,

Table 2 Selected bond lengths (Å) and angles (°) for complexes **1–4**

	1·0.5H_2O	**2**·0.32H_2O	**3**	**4**·0.5MeOH
Mn1–O3–Mn2	120.73(8)	119.50(1)	120.00(1)	120.20(9)
O2–Mn1–O3	95.57(7)	95.86(9)	95.35(9)	95.15(7)
N1–Mn2–O3	90.35(7)	91.87(9)	91.43(9)	91.63(7)
Mn1–O2–N1–Mn2	8.40(2)	13.60(2)	12.90(2)	8.80(2)
Mn1···Mn2	3.1349(5)	3.1136(6)	3.1230(6)	3.1215(5)
Mn1–O3	1.792(1)	1.787(2)	1.787(2)	1.782(1)
Mn2–O3	1.814(2)	1.818(2)	1.820(2)	1.819(2)
Mn1–O2	1.903(2)	1.905(2)	1.898(2)	1.888(2)
Mn2–N1	2.025(2)	2.034(2)	2.033(2)	2.019(2)
Mn1–N5	2.063(2)	2.059(2)	2.074(2)	2.059(2)
Mn2–O1	1.886(2)	1.873(2)	1.870(2)	1.873(2)
Mn1–N2	2.163(3)	2.166(3)	2.168(3)	2.161(2)
Mn2–N6	2.241(2)	2.245(2)	2.251(2)	2.221(2)
Mn1–N3	2.264(2)	2.259(3)	2.259(2)	2.270(2)
Mn2–N8	2.218(2)	2.214(3)	2.281(2)	2.207(2)
Mn1–N4	2.250(2)	2.242(2)	2.265(3)	2.252(2)
Mn2–N7	2.314(2)	2.282(2)	2.218(2)	2.239(2)

of 0.1 T over the 5 to 300 K temperature (T) range. The experimental results are shown in Fig. 2 in the form of the $\chi_M T$ product, where $\chi = M/B$ and M is the magnetisation of the sample.

At 300 K, the $\chi_M T$ products of **1** and **4**, have values of 4.87 and 4.90 cm^3 mol^{-1} K, respectively, significantly lower than the expected spin-only value of 6 cm^3 mol^{-1} K (for g = 2.0) for the uncorrelated ions. This is an indication of sizeable antiferromagnetic coupling between the Mn^{III} centres in **1** and **4**. For **3**, the $\chi_M T$ product at 300 K has a value of 5.54 cm^3 mol^{-1} K, again lower than the non-interacting-ions contribution, pointing towards the existence of an antiferromagnetic interaction between the Mn^{III} centres in **3**, as for **1** and **4**, but of lower magnitude. For **2**, the $\chi_M T$ product at 300 K has a value of 6.33 cm^3 mol^{-1} K, this time higher than the spin-only value, suggesting the existence of a ferromagnetic interaction between the Mn^{III} centres in **2**. On cooling, the $\chi_M T$ products of **1**, **3** and **4** drop, reaching 0.09, 0.20 and 0.10 cm^3 mol^{-1} K at 5 K, respectively. This behaviour is indicative of antiferromagnetic exchange between the Mn^{III} centres. In contrast, the $\chi_M T$ product of **2** first increases on cooling, reaching 6.84 cm^3 mol^{-1} K at 15 K, before decreasing to reach 6.38 cm^3 mol^{-1} K at 5 K. We have employed the isotropic spin-Hamiltonian (1) to model the temperature dependence of the $\chi_M T$ product of all four complexes:

$$\hat{H}_{iso} = -2J\hat{S}_1 \cdot \hat{S}_2 + \mu_B Bg(\hat{S}_1 + \hat{S}_2) \quad (1)$$

where the indices 1 and 2 refer to the two Mn^{III} centres, J is the isotropic exchange interaction parameter, $\hat{S}$ is a spin operator, μ_B is the Bohr magneton and g is the g-factor of Mn^{III}, assumed to be isotropic and equal to 2.00. Spin-Hamiltonian (1) was fitted to the experimental data by use of the Levenberg–Marquardt algorithm.[68] To extract J by use of spin-Hamiltonian (1) we fitted the experimental data only down to 20 K to avoid anisotropy terms not included in spin-Hamiltonian (1) that may become important at lower temperatures. This resulted in the best-fit parameters: J = −4.94, +0.29, −3.87, −5.17 cm^{-1}, for **1–4**, respectively. The obtained best-fit $\chi_M T$ product curves are shown as solid lines in Fig. 2. Thus, the ground spin-state of complexes **1**, **3** and **4** is a spin singlet, whereas the ground spin-state of complex **2** is an S = 4 state.

To better determine the low temperature magnetic properties of **2**, variable-temperature-variable-field (VTVB) magnetisation data were collected on polycrystalline samples of **2** (Fig. 2, inset) in the temperature and field ranges 2 to 7 K and 0.5 to 7.0 T. For the fitting of the VTVB magnetisation data of **2**, we used spin-Hamiltonian (2):

$$\hat{H}_{aniso} = \hat{H}_{iso} + \sum_{i=1,2} D_i(\hat{S}_{z,i}^2 - S_i(S_i+1))/3 \quad (2)$$

where $\hat{H}_{iso}$ refers to spin-Hamiltonian (1), D is the uniaxial anisotropy parameter and S the total spin of Mn^{III} (S = 2). Spin-Hamiltonian (2) was fitted to the experimental data by use of the simplex algorithm,[68] to give the best-fit parameter D_{Mn} = −1.9 cm^{-1}. Here we have assumed that the two Mn^{III} centres are characterised by the same D_{Mn}, even though **2** is asymmetric. This is clearly an approximation, justified however by the fact that D_{Mn} is determined by interpretation of the thermodynamic VTVB magnetisation data.

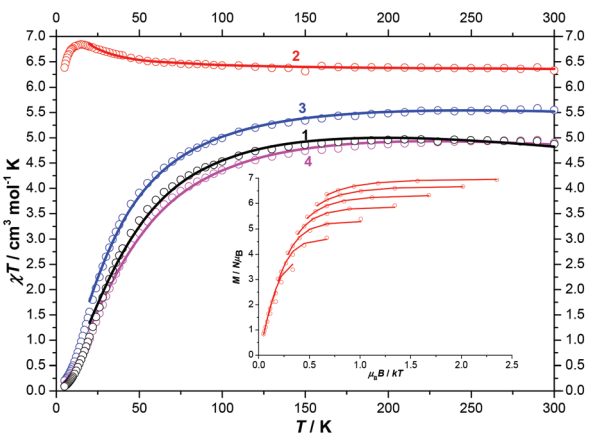

Fig. 2 Plot of $\chi_M T$ *vs.* T for complexes **1–4**. Inset: VTVB magnetisation data of **2**. Best-fit curves are shown as solid lines. See text for details.

Theoretical studies

Theoretical studies have been carried out in order to examine and understand the variation in the strength of exchange coupling in complexes **1–4**. The DFT computed J values are −5.97 cm^{-1}, −2.40 cm^{-1}, −5.30 cm^{-1}, −7.21 cm^{-1} for complexes **1–4**, respectively. All the exchange interactions are found to be antiferromagnetic in nature. The computed J values are in agreement with experiment, except in the case of complex **2** where the wrong sign has been predicted. Although B3LYP calculations often yield good numerical estimates of the exchange interactions, we note that J_{AF} (the antiferromagnetic contribution to the net exchange) is commonly overestimated. This is particularly true for complexes containing

Mn^{III} ions,[69,70] and in this set of complexes the magnitude of the antiferromagnetic exchange is overestimated by more than one wavenumber in all cases. As the ferromagnetic exchange in complex **2** is extremely weak, the overestimation of J_{AF} leads to a net antiferromagnetic J value. The calculations do however reflect the observed experimental trend of increasing J_{AF} contribution **4** > **1** > **3** > **2**. To gain insight into the electronic origin of the exchange we have analysed the molecular orbitals (MOs), spin densities and have computed the overlap integrals between pairs of magnetic orbitals. Our earlier theoretical studies on $\{Mn^{III}{}_2(OR)_2\}$ dimers,[70] which correlated the magnitude of the pairwise exchange interaction to the relative orientation of the Jahn–Teller axes, would suggest that complexes **1–4** are type I dimers: in **1–4** the Jahn–Teller axes on the two Mn^{III} ions are parallel to each other, suggesting an antiferromagnetic interaction. The computed overlap integral values for complexes **1–4** are given in Table S1 of the ESI.‡ Analysis of the MO and the overlap integrals suggest the following pairs of interactions to be the most dominant, thus deciding the sign and strength of J in all four complexes:

$$J_{net} \approx J_{AF}(d_{xy}|\pi^*|d_{xy}) + J_{AF}(d_{xz}|\pi^*|d_{xz}) + J_{AF}(d_{yz}|\pi^*|d_{yz}) + 2J_F(d_{xy}|\pi^*|d_{x^2-y^2})$$

In all four cases, a significant interaction between d_{xy}–d_{xy}, d_{xz}–d_{xz} and d_{yz}–d_{yz} has been observed, along with a significant d_{xy}–$d_{x^2-y^2}$ cross-interaction which contributes to ferromagnetic coupling. The d_{xy}–d_{xy} overlap is directly related to the Mn···Mn distance and is almost constant for all four complexes, while the d_{xz}–d_{xz} interaction is mediated through the μ-oxo bridge (Fig. 3A) and its strength is related to both the Mn–O distance and the Mn–O–Mn angle.[70] The d_{yz}–d_{yz} interaction (Fig. 3A) on the other hand is propagated through the Mn–O–N–Mn bridge and its dihedral angle significantly affects this overlap, *i.e.* the d_{yz}–d_{yz} overlap is prominent for lower Mn–N–O–Mn dihedral angles and disappears for larger dihedral angles (Table S1‡).

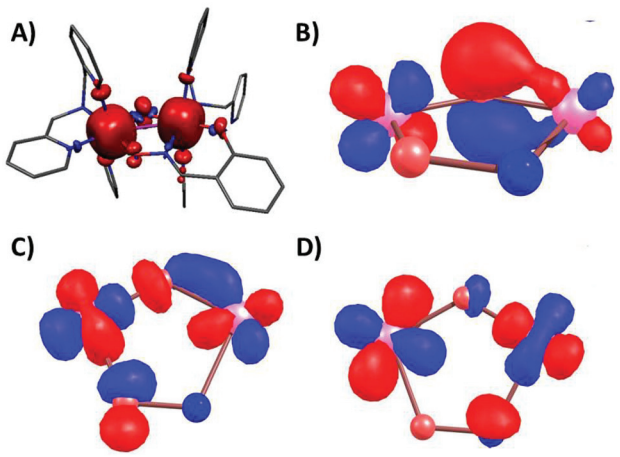

Fig. 3 (A) Computed spin density plot for complex **1**. Qualitative MO diagram computed for complex **2**: (B) d_{xz} orbital; (C) $d_{x^2-y^2}$ orbital (alpha); (D) $d_{x^2-y^2}$ orbital (beta). For (B)–(D) the ligands and other atom contributions are removed for clarity. See Fig. S2‡ for the complete picture.

The d_{xy}–$d_{x^2-y^2}$ cross interaction routes through both μ-oxo and Mn–N–O–Mn bridges (see Fig. 3C–D for alpha and beta counter parts). Since the d_{xy} and $d_{x^2-y^2}$ orbitals are π and σ type orbitals respectively, a twist in the Mn–O–N–Mn dihedral angle increases this overlap while a smaller dihedral diminishes the cross interaction. Thus, for the most antiferromagnetic complex, **4**, a significant d_{xz}–d_{xz} overlap (shortest Mn–O distance), a significant d_{yz}–d_{yz} overlap (smallest Mn–O–N–Mn dihedral angle) and a smaller d_{xy}–$d_{x^2-y^2}$ overlap has been detected, while for complex **2** the d_{xy}–$d_{x^2-y^2}$ interaction is the most prominent with a significant decrease in the d_{yz}–d_{yz} overlap.

The spin density plot computed for complex **1** is shown in Fig. 3 (see Fig. S1‡ for plots for **2–4**). The Mn^{III} ions are found to possess three unpaired electrons in the t_{2g} orbitals (metal π-type) which promote a spin polarization mechanism, and one unpaired electron in an e_g orbital (metal σ type) favouring a spin delocalization mechanism. As a whole therefore, a combination of both spin delocalization and spin polarization mechanisms is evident, as also observed in the previously studied $\{Mn^{III}{}_2(OR)_2\}$ dimers.[70] The ligand atoms in the direction of d_{z^2}-orbital, *i.e.* along the Jahn–Teller axes, are found to experience a spin delocalization mechanism as can be visualized from the red spin densities on these atoms in Fig. 3. Along the direction of t_{2g} orbitals of the ligand atoms (in the equatorial positions) there is a mixture of spin delocalization and spin polarization mechanisms. Due to the oxime coordination (N *vs.* O donor) the spin densities on the two Mn^{III} ions are slightly different (Table S2‡). In all complexes the oxime-N(O) atoms have negative (positive) spin densities, with the smallest (highest) value found for complex **2**, indicating that polarization(delocalization) through the Mn–N–O–Mn bridge is least efficient due to the twisting of this moiety, in accord with the orbital model proposed above.

One of the key parameters that is found to vary across the series is the Mn–N–O–Mn dihedral (torsion) angle, since all other parameters which are likely to affect the exchange interactions, remain nearly constant. To probe the role of the dihedral angle in determining the sign of the exchange interaction we have developed a theoretical magneto-structural correlation for complex **1**. Earlier theoretical and experimental correlations developed for oxime-based $[Mn_6]$ and $[Mn_3]$ single-molecule magnets revealed that the Mn–O–N–Mn torsion angle was the key/dominant parameter for determining the nature and magnitude of the exchange interaction.[37–39] To understand the effect of this parameter on complexes **1–4**, the torsion angle in complex **1** has been varied from 0 to 30° (Fig. 4). A linear correlation is evident for this parameter, with the experimental data points for **1–4** fitting nicely on this graph. The magnitude of J is found to vary significantly as the dihedral angle is altered. As the dihedral angle increases the AF exchange decreases and a switch to ferromagnetic exchange is observed at approximately 18°, due to a decrease in the d_{yz}–d_{yz} overlap and an increase in number of cross-interactions (Table S3‡). The overlap integral and computed trend correlates well with the proposed magnetic coupling.

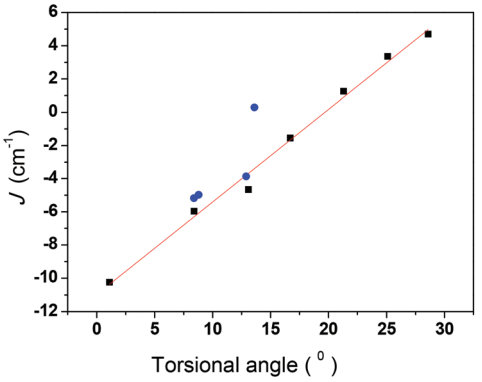

Fig. 4 Magneto-structural correlation developed by varying the Mn–N–O–Mn angle in **1**; blue circles represent the experimental *J* values for **1–4**.

Conclusions

The reaction between a Mn^{II} salt, a phenolic oxime and the tetradentate chelate tpa in a basic alcoholic solution affords a small family of cationic dimers of general formula $[Mn^{III}_2O(R\text{-sao})(tpa)_2]^{2+}$ in which the two Mn^{III} ions are bridged by one $\mu\text{-}O^{2-}$ ion and the –N–O– moiety of the oxime. Changing the R-group on the oxime ligand enforces subtle changes in the geometry of the magnetic core of the molecules as evidenced by a weakening of the AF contribution to the exchange interaction and the presence of dominant F exchange in one family member. A theoretical magneto-structural correlation reveals a linear relationship between the Mn–O–N–Mn angle and the magnitude of *J*, with the larger angles enforcing a decrease in J_{AF}.

Acknowledgements

HOS and WPB acknowledge the financial support from the Brazilian agencies Conselho Nacional de Desenvolvimento Científico e Tecnológico (CNPq) and Fundação de Amparo à Pesquisa do Estado de Minas Gerais (FAPEMIG). EKB and SP thank the EPSRC and Leverhulme Trust, and the Danish Natural Science Research Council (FNU) for a Sapere Aude Fellowship (10-081659), respectively. GR and TR acknowledge financial support from the Government of India through the Department of Science and Technology (SR/S1/IC-41/2010; SR/NM/NS-1119/2011), and the Indian Institute of Technology Bombay for computing time.

Notes and references

1 M. Ganzhorn, S. Klyatskaya, M. Ruben and W. Wernsdorfer, *Nat. Nanotechnol.*, 2013, **8**, 165.
2 R. Vincent, S. Klyatskaya, M. Ruben and W. Wernsdorfer, *Nature*, 2012, **488**, 357.
3 M. L. Baker, T. Guidi, S. Carretta, J. Ollivier, H. Mutka, H.-U. Güdel, G. A. Timco, E. J. L. McInnes, G. Amoretti, R. E. P. Winpenny and P. Santini, *Nat. Phys.*, 2012, **8**, 906.
4 C. F. Lee, D. A. Leigh, R. G. Pritchard, D. Schultz, S. J. Teat, G. A. Timco and R. E. P. Winpenny, *Nature*, 2009, **458**, 314.
5 M. Mannini, F. Pineider, C. Danieli, F. Totti, L. Sorace, P. Sainctavit, M. A. Arrio, E. Otero, L. Joly, J. C. Cezar, A. Cornia and R. Sessoli, *Nature*, 2010, **468**, 417.
6 M. Mannini, F. Pineider, P. Sainctavit, C. Danieli, E. Otero, C. Sciancalepore, A. M. Talarico, M. A. Arrio, A. Cornia, G. Gatteschi and R. Sessoli, *Nat. Mater.*, 2009, **8**, 194.
7 J. D. Rinehardt, M. Fang, W. J. Evans and J. R. Long, *Nat. Chem.*, 2011, **3**, 538.
8 J. D. Rinehardt and J. R. Long, *Chem. Sci.*, 2011, **11**, 2078.
9 R. Ruamps, R. Maurice, L. Batchelor, M. Boggio-Pasqua, R. Guillot, A. L. Barra, J. J. Liu, E. Bendeif, S. Pillet, S. Hill, T. Mallah and N. Guihery, *J. Am. Chem. Soc.*, 2013, **135**, 3017.
10 S. Hill, S. Datta, J. Liu, R. Inglis, C. J. Milios, P. L. Feng, J. J. Henderson, E. del Barco, E. K. Brechin and D. N. Hendrickson, *Dalton Trans.*, 2010, **39**, 4693.
11 J. Luzon, K. Bernot, I. J. Hewitt, C. E. Anso, A. K. Powell and R. Sessoli, *Phys. Rev. Lett.*, 2008, **100**, 247205.
12 J. J. Baldovi, S. Cardona-Serra, J. M. Clemente-Juan, E. Coronado and A. Gaita-Arino, *Chem. Sci.*, 2013, **4**, 938.
13 R. Bagai and G. Christou, *Chem. Soc. Rev.*, 2009, **38**, 1011.
14 G. E. Kostakis, I. J. Hewitt, A. M. Ako, V. Mereacre and A. K. Powell, *Philos. Trans. R. Soc., A*, 2010, **368**, 1509.
15 K. S. Murray, *Aust. J. Chem.*, 2009, **62**, 1081.
16 M. Nakano and H. Oshio, *Chem. Soc. Rev.*, 2011, **40**, 3239.
17 L. Engelhardt and M. Luban, *Dalton Trans.*, 2010, **39**, 4687.
18 J. Schnack, *Dalton Trans.*, 2010, **39**, 4677.
19 U. Kortz, A. Müller, J. van Slageren, J. Schnack, N. S. Dalal and M. Dressel, *Coord. Chem. Rev.*, 2009, **253**, 2315.
20 N. Hoshino, M. Nakano, H. Nojiri, W. Wernsdorfer and H. Oshio, *J. Am. Chem. Soc.*, 2009, **131**, 15100.
21 S. Loth, S. Baumann, C. P. Lutz, D. M. Eigler and A. J. Heinrich, *Science*, 2012, **335**, 196.
22 M. N. Leuenberger and D. Loss, *Nature*, 2001, **410**, 789.
23 L. Bogani and W. Wernsdorfer, *Nat. Mater.*, 2008, **7**, 179.
24 C. J. Wedge, G. A. Timco, E. T. Spielberg, R. E. George, F. Tuna, S. Rigby, E. J. L. McInnes, R. E. P. Winpenny, S. J. Blundell and A. Ardavan, *Phys. Rev. Lett.*, 2012, **108**, 107204.
25 M. Evangelisti, F. Luis, L. J. de Jongh and M. Affronte, *J. Mater. Chem.*, 2006, **16**, 2534.
26 M. Evangelisti and E. K. Brechin, *Dalton Trans.*, 2010, **39**, 4672.
27 *Magneto-Structural Correlations in Exchange-Coupled Systems*, ed. D. Gatteschi, O. Kahn and R. D. Willet, D. Reidel, Dordrecht, 1985.
28 S. S. Tandon, L. K. Thompson, M. E. Manuel and J. N. Bridson, *Inorg. Chem.*, 1994, **33**, 5555.
29 W. E. Hatfield, *Comments Inorg. Chem.*, 1981, **1**, 105.
30 H. Weihe and H. Güdel, *J. Am. Chem. Soc.*, 1997, **119**, 6539.
31 F. Neese, *J. Am. Chem. Soc.*, 2006, **128**, 10213.
32 T. Cauchy, E. Ruiz and S. Alvarez, *J. Am. Chem. Soc.*, 2006, **128**, 15722.
33 E. Ruiz, *Struct. Bonding*, 2004, **113**, 71.

34 O. Kahn and B. Briat, *J. Chem. Soc., Faraday Trans. 2*, 1976, **72**, 268.
35 G. Christou, *Acc. Chem. Res.*, 1989, **22**, 328.
36 A. G. Smith, P. A. Tasker and D. J. White, *Coord. Chem. Rev.*, 2003, **241**, 61; P. Chaudhuri, *Coord. Chem. Rev.*, 2003, **243**, 143; C. J. Milios, T. C. Stamatatos and S. P. Perlepes, *Polyhedron*, 2006, **25**, 134.
37 R. Inglis, C. J. Milios, L. F. Jones and E. K. Brechin, *Chem. Commun.*, 2012, **48**, 181; C. J. Milios, S. Piligkos and E. K. Brechin, *Dalton Trans.*, 2008, 1809.
38 C. J. Milios, R. Inglis, A. Vinslava, R. Bagai, W. Wernsdorfer, S. Parsons, S. P. Perlepes, G. Christou and E. K. Brechin, *J. Am. Chem. Soc.*, 2007, **129**, 12505; C. J. Milios, A. Vinslava, W. Wernsdorfer, A. Prescimone, P. A. Wood, S. Parsons, S. P. Perlepes, G. Christou and E. K. Brechin, *J. Am. Chem. Soc.*, 2007, **129**, 6547; C. J. Milios, A. Vinslava, W. Wernsdorfer, S. Moggach, S. Parsons, S. P. Perlepes, G. Christou and E. K. Brechin, *J. Am. Chem. Soc.*, 2007, **129**, 2754; C. J. Milios, A. Vinslava, P. A. Wood, S. Parsons, W. Wernsdorfer, G. Christou, S. P. Perlepes and E. K. Brechin, *J. Am. Chem. Soc.*, 2007, **129**, 8.
39 R. Inglis, J. Bendix, T. Brock-Nannestad, H. Weihe, E. K. Brechin and S. Piligkos, *Chem. Sci.*, 2010, **1**, 631; R. Inglis, S. M. Taylor, L. F. Jones, G. S. Papaefstathiou, S. P. Perlepes, S. Datta, S. Hill, W. Wernsdorfer and E. K. Brechin, *Dalton Trans.*, 2009, 9157; R. Inglis, L. F. Jones, C. J. Milios, S. Datta, A. Collins, S. Parsons, W. Wernsdorfer, S. Hill, S. P. Perlepes, S. Piligkos and E. K. Brechin, *Dalton Trans.*, 2009, 3403; R. Inglis, L. F. Jones, G. Karotsis, A. Collins, S. Parsons, S. P. Perlepes, W. Wernsdorfer and E. K. Brechin, *Chem. Commun.*, 2008, 5924; S. Piligkos, J. Bendix, H. Weihe, C. J. Milios and E. K. Brechin, *Dalton Trans.*, 2008, 2277; J. Cano, T. Cauchy, E. Ruiz, C. J. Milios, C. C. Stoumpos, T. C. Stamatatos, S. P. Perlepes, G. Christou and E. K. Brechin, *Dalton Trans.*, 2008, 234.
40 M. Manoli, R. Inglis, M. J. Manos, V. Nastopoulos, W. Wernsdorfer, E. K. Brechin and A. J. Tasiopoulos, *Angew. Chem., Int. Ed.*, 2011, **50**, 4441.
41 E. Houton, S. M. Taylor, C. C. Beedle, J. Cano, S. Piligkos, S. Hill, A. G. Ryder, E. K. Brechin and L. F. Jones, *Dalton Trans.*, 2012, **41**, 8340; R. Inglis, E. Houton, J. Liu, A. Prescimone, J. Cano, S. Piligkos, S. Hill, L. F. Jones and E. K. Brechin, *Dalton Trans.*, 2011, **40**, 9999.
42 G. Rigaux, R. Inglis, S. Morrison, A. Prescimone, C. Cadiou, M. Evangelisti and E. K. Brechin, *Dalton Trans.*, 2011, **40**, 4797.
43 R. J. Parker, L. Spiccia, B. Moubaraki, K. S. Murray, B. W. Skelton and A. H. White, *Inorg. Chim. Acta*, 2000, **300**, 922.
44 A. Rodriguez-Fortea, P. Alemany, S. Alvarez, E. Ruiz, A. Scuiller, C. Decroix, V. Marvaud, J. Vaissermann, M. Verdaguer, I. Rosenman and M. Julve, *Inorg. Chem.*, 2001, **40**, 5868.
45 M. E. Helton, P. Chen, P. P. Paul, Z. Tyeklar, R. D. Sommer, L. N. Zakharov, A. L. Rheingold, E. I. Solomon and K. D. Karlin, *J. Am. Chem. Soc.*, 2003, **125**, 1160.
46 R. A. Leising, J. H. Kim, M. A. Perez and L. Que, *J. Am. Chem. Soc.*, 1993, **115**, 9524.
47 J. Kim, E. Larka, E. C. Wilkinson and L. Que, *Angew. Chem., Int. Ed. Engl.*, 1995, **34**, 2048.
48 N. J. Robertson, M. J. Carney and J. A. Halfen, *Inorg. Chem.*, 2003, **42**, 6876.
49 D. J. Hodgson, M. H. Zietlow, E. Pedersen and H. Toftlund, *Inorg. Chim. Acta*, 1988, **149**, 111.
50 B. G. Gafford and R. A. Holwerda, *Inorg. Chem.*, 1989, **28**, 60.
51 B. G. Gafford, R. E. Marsh, W. P. Schaefer, J. H. Zhang, C. J. O'Connor and R. A. Holwerda, *Inorg. Chem.*, 1990, **29**, 4652.
52 B. Tong, S. C. Chang, E. E. Carpenter, C. J. O'Connor, J. O. Lay and R. E. Norman, *Inorg. Chim. Acta*, 2000, **300**, 855.
53 L. Yang, Y. Peng, F. Bian, S. P. Yan, D. Z. Liao, P. Cheng and Z. H. Jiang, *J. Coord. Chem.*, 2003, **56**, 961.
54 D. K. Towle, C. A. Botsford and D. J. Hodgson, *Inorg. Chim. Acta*, 1988, **141**, 167.
55 B.-K. Shin, Y. Kim, M. Kim and J. Han, *Polyhedron*, 2007, **26**, 4557.
56 B. K. Shin, M. Kim and J. Han, *Polyhedron*, 2010, **29**, 2560.
57 Y. Zang, J. Kim, Y. Dong, E. C. Wilkinson, E. H. Appelman and L. Que, *J. Am. Chem. Soc.*, 1997, **119**, 4197.
58 L. Que and Y. H. Dong, *Acc. Chem. Res.*, 1996, **29**, 190.
59 M. Costas, K. Chen and L. Que, *Coord. Chem. Rev.*, 2000, **200**, 517.
60 W. R. Dunstan and T. A. Henry, *J. Chem. Soc. Trans.*, 1899, **75**, 66.
61 L. Palatinus and G. Chapuis, *J. Appl. Crystallogr.*, 2007, **40**, 786.
62 G. M. Sheldrick, *Acta Crystallogr., Sect. A: Fundam. Crystallogr.*, 2008, **64**, 112–122.
63 A. D. Becke, *J. Chem. Phys.*, 1993, **98**, 5648.
64 A. Schafer, H. Horn and R. Ahlrichs, *J. Chem. Phys.*, 1992, 97; A. Schafer, C. Huber and R. Ahlrichs, *J. Chem. Phys.*, 1994, **100**, 5829.
65 M. J. Frisch, G. W. Trucks, H. B. Schlegel, G. E. Scuseria, M. A. Robb, J. R. Cheeseman, G. Scalmani, V. Barone, B. Mennucci, G. A. Petersson, H. Nakatsuji, M. Caricato, X. Li, H. P. Hratchian, A. F. Izmaylov, J. Bloino, G. Zheng, J. L. Sonnenberg, M. Hada, M. Ehara, K. Toyota, R. Fukuda, J. Hasegawa, M. Ishida, T. Nakajima, Y. Honda, O. Kitao, H. Nakai, T. Vreven, J. A. Montgomery Jr., J. E. Peralta, F. Ogliaro, M. Bearpark, J. J. Heyd, E. Brothers, K. N. Kudin, V. N. Staroverov, R. Kobayashi, J. Normand, K. Raghavachari, A. Rendell, J. C. Burant, S. S. Iyengar, J. Tomasi, M. Cossi, N. Rega, J. M. Millam, M. Klene, J. E. Knox, J. B. Cross, V. Bakken, C. Adamo, J. Jaramillo, R. Gomperts, R. E. Stratmann, O. Yazyev, A. J. Austin, R. Cammi, C. Pomelli, J. W. Ochterski, R. L. Martin, K. Morokuma, V. G. Zakrzewski, G. A. Voth, P. Salvador,

J. J. Dannenberg, S. Dapprich, A. D. Daniels, O. Farkas, J. B. Foresman, J. V. Ortiz, J. Cioslowski and D. J. Fox, *GAUSSIAN 09 (Revision A.02)*, Gaussian, Inc., Wallingford, CT, 2009.

66 L. Noodleman, *J. Chem. Phys.*, 1981, **74**, 5737.

67 E. Ruiz, S. Alvarez, J. Cano and P. Alemany, *J. Comput. Chem.*, 1999, **20**, 1391; E. Ruiz, A. Rodriguez-Fortea, J. Cano, S. Alvarez and P. Alemany, *J. Comput. Chem.*, 2003, **24**, 982; G. Rajaraman, J. Cano, E. K. Brechin and E. J. L. McInnes, *Chem. Commun.*, 2004, 1476; P. Christian, G. Rajaraman, A. Harrison, J. J. W. McDouall, J. Raftery and R. E. P. Winpenny, *Dalton Trans.*, 2004, 2550; G. Rajaraman, M. Murugesu, E. C. Sanudo, M. Soler, W. Wernsdorfer, M. Helliwell, C. Muryn, J. Raftery, S. J. Teat, G. Christou and E. K. Brechin, *J. Am. Chem. Soc.*, 2004, **126**, 15445; S. Sasmal, S. Hazra, P. Kundu, S. Dutta, G. Rajaraman, E. C. Sanudo and S. Mohanta, *Inorg. Chem.*, 2011, **50**, 7257.

68 W. H. Press, S. A. Teukolsky, W. T. Vetterling and B. P. Flannery, *Numerical Recipes in C: The Art of Scientific Computing*, Cambridge University Press, Cambridge, 2nd edn, 1992.

69 G. Rajaraman, E. C. Sanudo, M. Helliwell, S. Piligkos, W. Wernsdorfer, G. Christou and E. K. Brechin, *Polyhedron*, 2005, **24**, 2450.

70 N. Berg, T. Rajeshkumar, S. M. Taylor, E. K. Brechin, G. Rajaraman and L. F. Jones, *Chem.–Eur. J.*, 2012, **18**, 5906.